THE AMERICAN SOCIETY OF MECHANICAL ENGINEERS
345 E. 47 St., New York, N.Y. 10017

89-WA/DSC-38

On QFT-Type Controller Design for Maximizing the Size of a Persistent Disturbance

PETER ZENTGRAF and SUHADA JAYASURIYA
Lehrstuhl für Regelsysteme und Steuerungstechnik
Ruhr-Universität Bochum
D-4630 Bochum, West Germany
and
Department of Mechanical Engineering
Texas A&M University
College Station, TX 77843-3123

ABSTRACT

A frequency domain design methodology proposed in Jayasuriya and Franchek [1988] provides for the satisfaction of controller and state constraints in the presence of an unknown-but-bounded disturbance. The methodology is based on mapping the constraints expressed in the time domain into the frequency domain to determine a suitable target feedback system. An improvement of the methodology based on a geometric interpretation of the design constraints lends itself to an effective technique for determining the maximum bound on a persistent bounded disturbance. The geometric interpretation is made in terms of a family of well defined circles. A loop shaping procedure is also developed. The design methodology is applied to a fourteenth-order nuclear power plant model.

I. INTRODUCTION

In practical systems the control goal is often to keep state or output signals in certain predetermined bounds in the presence of various disturbances. A design technique that accounts for such performance requirements was recently proposed in Jayasuriya and Franchek [1988]. Specifically, they consider the problem of directly satisfying constraints on system states and bandwidth limits while maximizing the size of an allowable persistent bounded disturbance. The approach is based on frequency domain ideas. The time domain constraints on a linear time invariant system with unity feed back under the influence of a bounded disturbance are transformed into the frequency domain. Many important feedback issues, such as sensor noise and energy distribution, can be better seen in the time domain.

An improvement of the above methodology based on a geometric interpretation of the design constraints is the main focus of the present study. It is shown that the time domain constraints correspond to a family of closed loop circles with their common area of intersection displaying the allowed design region for the closed loop transfer function. From this circle family, a technique for determining the maximum tolerable disturbance is also derived. Moreover, design bounds on magnitude and phase are also generated for finding suitable loop transfer functions. The Bode plot and the Nichols chart are used as the primary tools for loop shaping.

The initial justification for the design methodology was on heuristic reasoning and simulation results. Recently, its basic assumptions have been justified theoretically (Jayasuriya, Zentgraf and Rabins [1990]). For disturbance rejection, Jayasuriya and Franchek [1988] argue that if the system can reject a step of a given height, it is likely to reject any disturbance signal whose amplitude is bounded by the step size. This reasoning was based on the fact that a step includes the slowest possible signal, a constant value, and the fastest possible signal, the initial impulse. Since then, it has been shown (Jayasuriya, Zentgraf and Rabins [1989]) that this is true if and only if the system transfer function is "strictly proper" and its impulse response does not change sign. Otherwise, a square wave signal can always be found to violate the time domain constraints.

Another contribution of this work is the investigation of the relation between a bounded step response in the time domain and the corresponding magnitude of the system transfer function. This completes the general justification of the methodology.

Section II gives the problem formulation and a theoretical justification, followed by the design method. A fourteenth-order model of a nuclear power plant is studied in section III using our design methodology. A summary of the results and conclusions are given in section IV.

II. PROBLEM FORMULATION AND DESIGN METHOD

Consider a linear, time invariant, single input, multiple output system (SIMO system) described by the following state equations

$$\dot{\mathbf{x}}(t) = \mathbf{A}\mathbf{x}(t) + \mathbf{B}u(t) + \mathbf{G}w(t) \tag{1}$$

$$\mathbf{y}(t) = \mathbf{H}\mathbf{x}(t) \tag{2}$$

where $\mathbf{x}(t) \in \mathbf{R}^m$ is the state vector, $u(t) \in \mathbf{R}^1$ is the scalar

Presented at the Winter Annual Meeting
San Francisco, California—December 10-15, 1989

control, $w(t) \epsilon \mathbf{R}^1$ is the scalar input disturbance and $\mathbf{y}(t) \epsilon \mathbf{R}^n$ is the output vector. The matrices **A**, **B**, **G** and **H** are of appropriate dimensions.

The output signals $y_l(t)$, $l = 1, 2, ...n$, the control variable $u(t)$ and the control rate $\dot{u}(t)$ have for all times the constant upper bound β_l, β_u and $\beta_{\dot{u}}$, respectively: $|y_l(t)| \leq \beta_l$, $|u(t)| \leq \beta_u$ and $|\dot{u}(t)| \leq \beta_{\dot{u}}$ for $t \epsilon [0, \infty)$. The design objective is to find a controller that keeps the system within the above prespecified bounds under a bounded disturbance signal $|w(t)| \leq \frac{1}{\alpha}$, $\alpha > 0$ for all times.

Laplace transforming (1) and (2) yields

$$\mathcal{L}[y_l(t)] = Y_l(s) = G_{lw}(s) \cdot W(s) + G_{lu}(s) \cdot U(s) \qquad (3)$$

where $\mathcal{L}[u(t)] = U(s)$, $\mathcal{L}[w(t)] = W(s)$, $G_{lu} = [\mathbf{H}(s\mathbf{I} - \mathbf{A})^{-1}\mathbf{B}]_l$, $l = 1, 2, \cdots, n$, and $G_{lw} = [\mathbf{H}(s\mathbf{I} - \mathbf{A})^{-1}\mathbf{G}]_l, l = 1, 2, \cdots, n$.

Using the output signal y_i for feedback yields the block diagram shown in Fig. 1. From that the following transfer functions can be written:

$$\frac{Y_i(s)}{W(s)} = \frac{G_{iw}(s)}{1 + L_o(s)} \qquad (4)$$

and

$$\frac{U(s)}{W(s)} = \frac{-G_{iw}(s)}{G_{iu}(s)} \cdot \frac{L_o(s)}{1 + L_o(s)} \qquad (5)$$

where

$$L_o(s) = G_c(s) \cdot G_{iu}(s) \qquad (6)$$

is the open loop transfer function.

The controller rate $\dot{U}(s) = s \cdot U(s)$ has the transfer function

$$\frac{\dot{U}(s)}{W(s)} = s \cdot \frac{U(s)}{W(s)} = s \cdot \frac{-G_{iw}(s)}{G_{iu}(s)} \cdot \frac{L_o(s)}{1 + L_o(s)} \qquad (7)$$

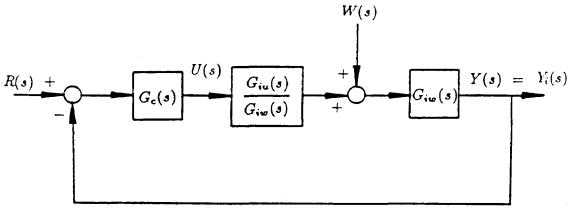

Fig. 1. Structure of a Feedback Control System with an Input Disturbance [1]

The transfer functions that relate the remaining states to the disturbance are obtained by substituting (5) in (3):

$$\frac{Y_j(s)}{W(s)} = G_{jw}(s) \cdot \left[1 + \frac{-G_{ju}(s) \cdot G_{iw}(s)}{G_{iu}(s) \cdot G_{jw}(s)} \cdot \frac{L_o(s)}{1 + L_o(s)}\right] \qquad (8)$$

where $j = 1, 2, ...n, j \neq i$.

The design goal is to find an $L_o(s)$ that guarantees $\beta_u \geq |u(t)|$, $\beta_{\dot{u}} \geq |\dot{u}(t)|$ and $\beta_l \geq |y_l(t)|$, $l = 1, 2, ...n$, up to a certain maximum disturbance for all times. If the impulse response of a strictly proper transfer function $G(s)$ does not change sign for $t \epsilon [0, \infty)$, the output signal $y(t)$ under the unknown-but-bounded input signal $|w(t)| \leq \frac{1}{\alpha}$ achieves its maximum for a step input $w(t) = \mathcal{L}^{-1}[\frac{1}{\alpha s}]$ (Jayasuriya, Zentgraf and Rabins [1990]). If the impulse response changes sign, a square wave signal with an appropriate switching depending on the location of the sign change can be found that yields a greater value for $y(t)$ than due to that of the step response. Since the impulse response is the time derivative of the step response, a sign switch on the impulse response corresponds to an oscillatory step response. Even if the response is oscillatory, a step yields the largest output if one can guarantee that the disturbance signal $w(t)$ is always either positive or negative, because the worst case cannot occur.

In further development of the approach the disturbance is treated as a step, and the assumption is justified later in time domain simulations.

II.1 Transforming Time Domain Bounds into the Frequency Domain:

The key to the method is mapping time domain bounds on the output signals and the controller to corresponding frequency domain bounds. Consider the bounded step response $h(t)$ due to a step input of height $\frac{1}{\alpha}$ (Fig. 2).

$$h(t) = \mathcal{L}^{-1}[H(s)] = \mathcal{L}^{-1}[G(s) \cdot \frac{1}{\alpha s}] \qquad (9)$$

Assume first $0 \leq h(t) \leq \beta$ for all times t, $t \epsilon [0, \infty)$; i.e., the system has no undershoot. This excludes systems with an odd number of positive zeros (Normiatsu [1961]).

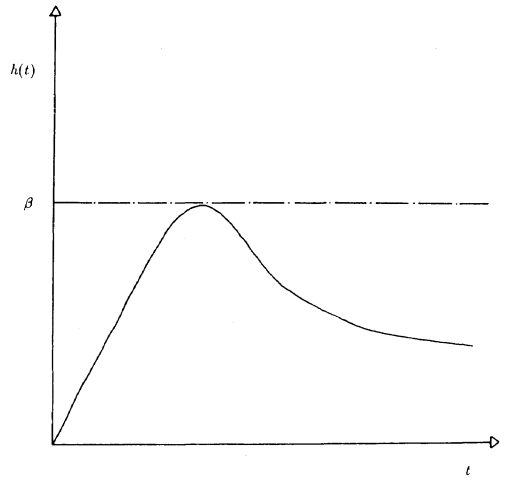

Fig. 2. Bounded Step Response $h(t)$

Substituting $s = j\omega$ in (9) the magnitude of the system $G(s)$ can be written as

$$|G(j\omega)| = |j\omega \cdot \alpha \cdot H(jw)| \qquad (10)$$

Using the Laplace Integral and estimating an upper bound for $|G(j\omega)|$ with the time domain bound β on $h(t)$ yields

$$\begin{aligned} |G(j\omega)| &\leq \alpha \cdot |j\omega \int_0^\infty \beta \cdot e^{-j\omega t}\, dt| \\ &= \alpha \cdot \beta \cdot |\frac{j\omega}{-j\omega} \cdot [e^{-j\omega\infty} - 1]| \\ &\leq 2 \cdot \alpha \cdot \beta \end{aligned} \qquad (11)$$

Now consider a step response with an undershoot where the sign change occurs at $t = t_1$. Again, the Laplace Integral can be written as

$$
\begin{aligned}
|G(j\omega)| &= \alpha \cdot |j\omega \int_0^{\infty} h(t) \cdot e^{-j\omega t}\, dt| \\
&= \alpha \cdot \{|j\omega \int_0^{t_1} h(t) \cdot e^{-j\omega t}\, dt \\
&+ j\omega \int_{t_1}^{\infty} h(t) \cdot e^{-j\omega t}\, dt|\} \qquad (12)
\end{aligned}
$$

Using the time domain bound β as upper bound on $|G(j\omega)|$ and triangle inequality yields

$$
\begin{aligned}
|G(j\omega)| &\leq \alpha \cdot \beta \cdot \{|[e^{-j\omega t_1} - 1]| + |[e^{-j\omega\infty} - e^{-j\omega t_1}]|\} \\
&\leq \alpha \cdot \beta \cdot \{\ 4\ \} \qquad (13)
\end{aligned}
$$

This means that the magnitude of a system $|G(j\omega)|$ is always upper bounded by $4 \cdot \alpha \cdot \beta$, if the step response due to a step input of height $\frac{1}{\alpha}$ is bounded by β. This is only sufficient, because unstable systems can be bounded in the frequency domain too. But violating the bound $4 \cdot \alpha \cdot \beta$ is sufficient for violating the bound on the step response. Thus the region below $4 \cdot \alpha \cdot \beta$ in the frequency domain is a necessary location for the amplitude of a system $|G(j\omega)|$ (Fig. 3)

Simulation results show that for certain systems $G(s)$, a violation of the time domain bound occurs for a smaller upper bound than $4 \cdot \alpha \cdot \beta$; therefore, a scale factor γ with $0 < \gamma \leq 4$ is introduced. The smallest necessary region in the frequency domain can now be described by

$$
|G(j\omega)| \leq \alpha \cdot \beta \cdot \gamma \qquad (14)
$$

Experiments show that for most systems $\gamma = 1$. For systems without undershoot, γ lies between 0 and 2; for systems $G(s)$ with an undershoot, γ may be even greater than 2, but not greater than 4; the latter case relaxes the frequency bound. This makes sense, because admitting an undershoot means also relaxing the time bound.

Thus, a time response $h(t)$ due to a step input with height $\frac{1}{\alpha}$ that stays within the bound $|h(t)| \leq \beta$ has a corresponding system transfer function $G(s)$ such that $|G(j\omega)| \leq \alpha \cdot \beta \cdot \gamma$ with γ as a system dependent constant where $0 \leq \gamma \leq 4$. A classification of transfer functions $G(s)$ by the value of γ is a current research topic.

The method also provides sharpness. Consider a stable system $G(s)$ that is saturating at a specific frequency the frequency domain upper $\alpha \cdot \beta \cdot \gamma$. Assume the step response does not saturate the time domain bound; then the height of the step input could be increased until saturation. But this implies a violation of the necessary frequency bound. Therefore, saturating the frequency bound yields saturation of the time bound.

II.2 Development of an Allowed Region in the Frequency Domain:
Bringing the transfer functions (4 - 8) into the form (12) yields:

$$
\alpha \cdot \beta_u \geq |\frac{U(s)}{W(s)}| \qquad (15)
$$

$$
\alpha \cdot \beta_{\dot{u}} \geq |\frac{\dot{U}(s)}{W(s)}| \qquad (16)
$$

$$
\alpha \cdot \beta_i \geq |\frac{Y_i(s)}{W(s)}| \qquad (17)
$$

$$
\alpha \cdot \beta_j \geq |\frac{Y_j(s)}{W(s)}| \qquad (18)
$$

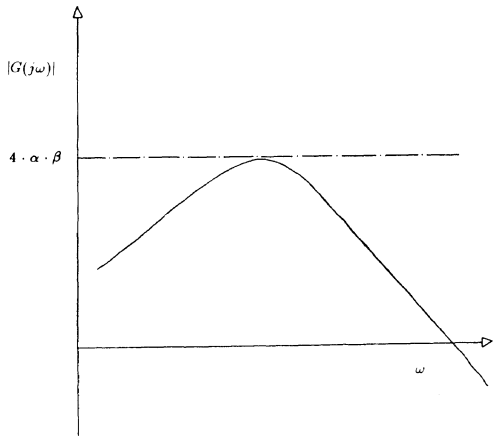

Fig. 3. Necessary Region of $|G(j\omega)|$ for a Bounded Step Response

Here, γ is assumed to be 1.

Substituting (4 - 8) in (15 - 18) and rearranging terms gives the inequalities for the yet unknown open loop transfer function $L_o(s)$ where $L_c(s) = \frac{L_o(s)}{1+L_o(s)}$:

$$
|1 + L_o(s)| \geq \frac{|G_{iw}(s)|}{\beta_i \cdot \alpha} \qquad (19)
$$

$$
|L_c(s)| \leq |\frac{-G_{iu}(s)}{G_{iw}(s)}| \cdot \beta_u \cdot \alpha \qquad (20)
$$

$$
|L_c(s)| \leq |\frac{-G_{iu}(s)}{G_{iw}(s)}| \cdot \frac{1}{|s|} \cdot \beta_{\dot{u}} \cdot \alpha \qquad (21)
$$

$$
|L_c(s) - \frac{G_{iu}(s) \cdot G_{jw}(s)}{G_{ju}(s) \cdot G_{iw}(s)}| \leq |\frac{G_{iu}(s) \cdot G_{jw}(s)}{G_{ju}(s) \cdot G_{iw}(s)}| \cdot \frac{\beta_j \cdot \alpha}{|G_{jw}(s)|} \qquad (22)
$$

It can be shown (Zentgraf [1989a]) that inequality (19) maps in the closed loop plane to

$$
|L_c(s) - 1| \leq |\frac{\alpha \cdot \beta_i}{G_{iw}(s)}| \qquad (23)
$$

All inequalities (20 - 23) represent at a constant frequency ω_ν "allowed circles" for $L_c(s)$ in the closed loop plane that meet constraints (15 - 18). The radii and center coordinates are summarized in Table 1. An arbitrary closed loop transfer function $L_c(s)$ that simultaneously meets all time domain constraints must necessarily lie within the common intersection area of the closed loop circles (Fig. 4) at each frequency.

Constraint Type	Radius	Center
Controller	$\lvert\frac{-G_{iu}(j\omega_\nu)}{G_{iw}(j\omega_\nu)}\rvert \cdot \beta_u \cdot \alpha$	0
Controller Rate	$\lvert\frac{-G_{iu}(j\omega_\nu)}{G_{iw}(j\omega_\nu)}\rvert \cdot \frac{1}{\lvert j\omega_\nu\rvert} \cdot \beta_{\dot{u}} \cdot \alpha$	0
Feedback State	$\lvert\frac{1}{G_{iw}(j\omega_\nu)}\rvert \cdot \beta_i \cdot \alpha$	1
Remaining State	$\lvert\frac{G_{iu}(j\omega_\nu) \cdot G_{jw}(j\omega_\nu)}{G_{iw}(j\omega_\nu) \cdot G_{ju}(j\omega_\nu)}\rvert \cdot \frac{1}{\lvert G_{jw}(j\omega_\nu)\rvert} \cdot \beta_j \cdot \alpha$	$\frac{G_{iu}(j\omega_\nu) \cdot G_{jw}(j\omega_\nu)}{G_{iw}(j\omega_\nu) \cdot G_{ju}(j\omega_\nu)}$

Table 1: Circles in the Closed Loop Plane as Necessary Locations for $L_c(s)$

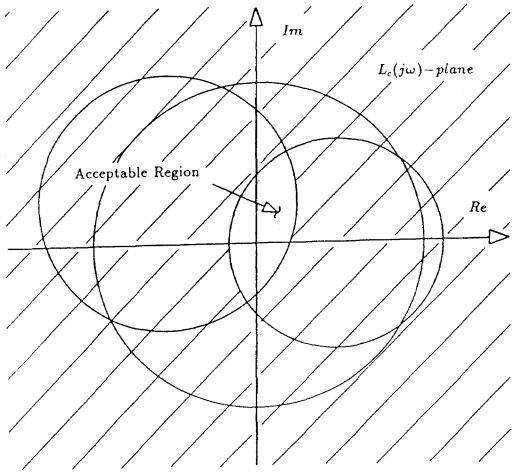

Fig. 4. Allowed Region for a Closed Loop Transfer Function $L_c(s)$ at $\omega = \omega_i$

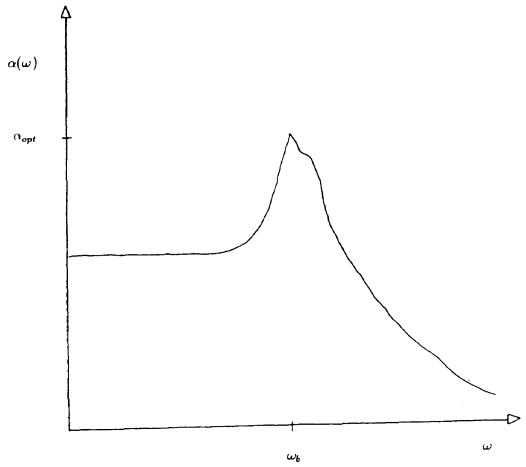

Fig. 5. Optimal Values of α over the Entire Frequency Range

II.3 Maximum Disturbance Rejection:

At a particular frequency, the maximum disturbance that can be rejected is achieved for a α_{opt} for which the common intersection area shrinks to a single, optimal point. An iterative algorithm has been developed (Zentgraf [1989b]) for computing the coordinates of this point and the corresponding value for $\alpha = \alpha_{opt}$. A typical plot of the function $\alpha_{opt}(\omega)$ is shown in (Fig. 5). The peak at frequency ω_b represents the theoretical maximum disturbance that can be rejected over the entire frequency range, which depends enirely on the system characteristics.

If the order of the numerator of the $G_{lw}(s)$ transfer function, $l = 1, 2, ...n$, is less than that of the characteristic polynomial, then

$$\lim_{\omega \to \infty} \alpha_{opt}(\omega) = 0 \tag{24}$$

This can be shown by formulating an upper bound on α_{opt}. Consider the origin. If it is included in all circles, their radii must have at least the same length as the distance of the centers from the origin, yielding the equation

$$\alpha_{up} = max \left[\frac{|G_{lw}(s)|}{\beta_l} \right], l = 1, 2, ...n \tag{25}$$

Clearly, this expression vanishes if the denominator has a higher order than the numerator (strictly proper), which is true in many physical systems. Note that the origin is also the center of the controller circle (Table 1) and therefore the controller constraint β_u and its rate constraint $\beta_{\dot{u}}$ do not impact the upper bound on α_{opt}.

II.4 Loop Shaping in the Frequency Domain:

The design procedure can be described as follows: First, the optimal points are plotted in a Bode diagram. Normally they correspond to a complex, high-order, nonrational transfer function termed the "optimal transfer function" $L_c(s)_{opt}$ because it gives the critical value for α, α_{opt} at every frequency ω. Second, the largest and smallest bounds on magnitude and phase on the allowed region (Fig. 4) for $\alpha_{design} = \alpha_{opt}$ are plotted in the Bode diagram (Fig. 6). This yields upper and lower bounds on

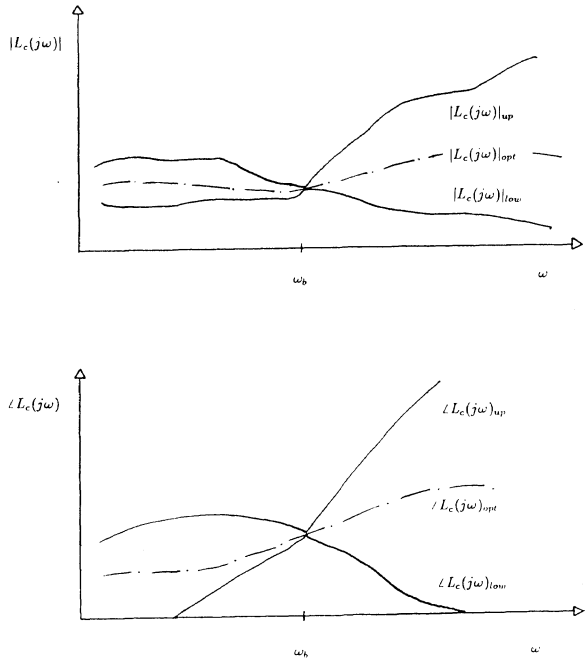

Fig. 6. Magnitude and Phase Bounds on $L_c(s)$

$L_c(s)$ for both magnitude and phase. Clearly, at the binding frequency ω_b they must meet. A closed loop transfer function $L_c(s)$ can now be designed that follows as closely as possible the optimal transfer function and stays within the bounds. In general it is difficult to meet magnitude and phase bounds with a low order system, since the approximation of the nonrational optimal transfer function generally requires high order. Hence the bounds are relaxed by increasing α_{design} to obtain lower order compensators.

II.5 Impact of the Choice of the Feedback Signal:

In Table 1 it is assumed that y_i is the feedback output. Now consider output y_k with $1 \leq k \leq n, k \neq i$ as the feedback.

This yields a new circle family (Table 2). Rotating the circles and stretching the whole plane give a conformal configuration with the same value for α_{opt} as before. Using the rotation angle $\angle \frac{G_{kw}(j\omega_\nu)\cdot G_{iu}(j\omega_\nu)}{G_{ku}(j\omega_\nu)\cdot G_{iw}(j\omega_\nu)}$ and the stretching factor $|\frac{G_{kw}(j\omega_\nu)\cdot G_{iu}(j\omega_\nu)}{G_{ku}(j\omega_\nu)\cdot G_{iw}(j\omega_\nu)}|$ gives the original circle family shown in Table 1. It proves that the choice of the feedback output does not affect the maximum disturbance rejection, so that an arbitrary output can be chosen for feedback with no restriction on the control performance.

Constraint Type	Radius	Center
Controller	$\lvert\frac{-G_{ku}(j\omega_\nu)}{G_{kw}(j\omega_\nu)}\rvert \cdot \beta_u \cdot \alpha$	0
Controller Rate	$\lvert\frac{-G_{ku}(j\omega_\nu)}{G_{kw}(j\omega_\nu)}\rvert \cdot \frac{1}{\lvert j\omega_\nu\rvert} \cdot \beta_u \cdot \alpha$	0
Feedback State	$\lvert\frac{1}{G_{kw}(j\omega_\nu)}\rvert \cdot \beta_k \cdot \alpha$	1
Remaining State	$\lvert\frac{G_{ku}(j\omega_\nu)\cdot G_{jw}(j\omega_\nu)}{G_{kw}(j\omega_\nu)\cdot G_{ju}(j\omega_\nu)}\rvert \cdot \frac{1}{\lvert G_{jw}(j\omega_\nu)\rvert} \cdot \beta_j \cdot \alpha$	$\frac{G_{ku}(j\omega_\nu)\cdot G_{jw}(j\omega_\nu)}{G_{kw}(j\omega_\nu)\cdot G_{iu}(j\omega_\nu)}$

Table 2: Circles in the Closed Loop Plane with Feedback Output y_k

II.6 Mapping of the Family of Closed Loop Circles into a Family of Open Loop Circles:

Because the mapping between open and closed loop plane is conformal, a family of open loop circles can be determined. Consider a circle in the closed loop plane with radius R_c and center (x_{mc}, y_{mc}) as shown in (Fig. 7) with the equation

$$(x_c - x_{mc})^2 + (y_c - y_{mc})^2 = R_c^2 \tag{26}$$

where x_c, y_c define the coordinate axes of the closed loop plane. The goal is to determine the corresponding radius R_o and center (x_{mo}, y_{mo}) of the open loop circle as a function of R_c and (x_{mc}, y_{mc}).

The open loop coordinates x_o, y_o are related to the closed loop coordinates x_c, y_c by

$$x_c + jy_c = \frac{x_o + jy_o}{1 + x_o + jy_o} \tag{27}$$

which yields

$$x_c = \frac{x_o + x_o^2 + y_o^2}{1 + 2\cdot x_o + x_o^2 + y_o^2} \tag{28}$$

$$y_c = \frac{y_o}{1 + 2\cdot x_o + x_o^2 + y_o^2} \tag{29}$$

Substituting (28) and (29) in (26) and rearranging terms gives

$$\begin{aligned} & [1 + 2\cdot x_o + x_o^2 + y_o^2]\cdot\{(x_o^2 + y_o^2)(1 - 2\cdot x_{mc} + x_{mc}^2 + y_{mc}^2) \\ + \; & x_o(-2\cdot x_{mc} + 2\cdot x_{mc}^2 + 2\cdot y_{mc}^2) + x_{mc}^2 + y_{mc}^2 - 2\cdot y_{mc}\cdot y_o\} \\ = \; & [1 + 2\cdot x_o + x_o^2 + y_o^2]\cdot R_c^2 \end{aligned} \tag{30}$$

Further rearranging of terms yields the circle equation of the corresponding open loop circle. Its radius and center are shown in Table 3. Also the inverse solution, the closed loop circle

Plane	Radius	Center(x-Coord.)	Center(y-Coord.)
Closed Loop	R_c	x_{mc}	y_{mc}
Open Loop	$\frac{R_c}{(1-x_{mc})^2 + y_{mc}^2 - R_c^2}$	$\frac{R_c^2 - (x_{mc}^2 + y_{mc}^2) + x_{mc}}{(1-x_{mc})^2 + y_{mc}^2 - R_c^2}$	$\frac{y_{mc}}{(1-x_{mc})^2 + y_{mc}^2 - R_c^2}$

Table 3: Open Loop Circle Corresponding to a Closed Loop Circle

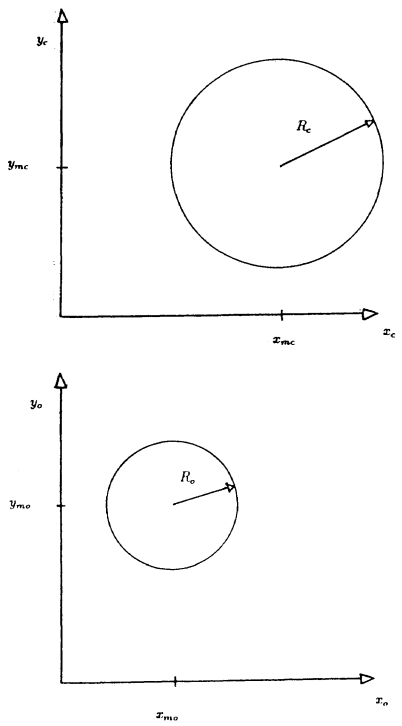

Fig. 7. Corresponding Circles in the Closed and Open Loop Plane

corresponding to an open loop circle with radius R_o and center (x_{mo}, y_{mo}), can be derived as shown in Table 4.

The inside of a circle in the closed loop plane that includes $1 + j0$ maps to the outside of the corresponding open loop circle, because $1 + j0$ in the closed loop plane maps to ∞ in the open loop plane. Hence the common area of intersection, the allowed region for a closed loop transfer function, of the family of closed loop circles does not necessarily map to a concave region in the open loop plane. If the common area of intersection includes $1 + j0$, then the allowed region in the closed loop plane is transformed into a forbidden region in the open loop plane. This fact is inconvenient to loop shape using a Bode plot. Furthermore, stability can be easily checked while designing a closed loop transfer function $L_c(s)$ instead of an open loop transfer function $L_o(s)$. Therefore the design process is made in the closed loop plane.

III. A NUCLEAR POWER PLANT EXAMPLE

A single-input multiple-output model of a simplified pressurized-water-reactor (PWR) type nuclear power plant is chosen (Parlos et al. [1988]) as a nontrivial example in order to demonstrate the design approach. The reactor equations are linearized at the operating points 10%, 20%, 50%, 70%, 90%, 100% and 110% of full power, yielding a fourteenth-order model with the form of (1) and (2).

The system has one input (rod position) and four output signals: average neutronics power deviation, average fuel temperature deviation, average hot-leg temperature deviation and the average primary coolant temperature deviation.

Plane	Radius	Center(x-Coord.)	Center(y-Coord.)
Open Loop	R_o	x_{mo}	y_{mo}
Closed Loop	$\frac{R_o}{(1+x_{mo})^2+y_{mo}^2-R_o^2}$	$\frac{-R_o^2+x_{mo}^2+y_{mo}{}^2-x_{mo}}{(1+x_{mo})^2+y_{mo}{}^2-R_o^2}$	$\frac{y_{mo}}{(1+x_{mo})^2+y_{mo}{}^2-R_o^2}$

Table 4: Closed Loop Circle Corresponding to an Open Loop Circle

The approach is detailed only for the model corresponding to 90% full power; the results for the complete model can be found in Zentgraf[1989b].

The transfer function model of the system corresponding to 90% of full power is given below.

$$G_{1u}(s) = \frac{22.0499}{\Delta(s)} \cdot (s + 2.4636 + j \cdot 0.1163)(s + 2.4636 - j \cdot 0.1163) \cdot (s + 0.4618 + j \cdot 0.2962)(s + 0.4618 - j \cdot 0.2962) \cdot (s + 0.2464)(s + 0.0769)s \quad (31)$$

$$G_{2u}(s) = \frac{3585.18}{\Delta(s)} \cdot (s + 2.4614 + j \cdot 0.1179)(s + 2.4614 - j \cdot 0.1179) \cdot (s + 0.4676 + j \cdot 0.2965)(s + 0.4676 - j \cdot 0.2965) \cdot (s + 0.0769)(s + 0.0074) \quad (32)$$

$$G_{3u}(s) = \frac{33.8301}{\Delta(s)} \cdot (s + 4.8012)(s + 4.7391)(s + 0.2906)(s + 0.2213) \cdot (s + 0.0769) \quad (33)$$

$$G_{4u}(s) = \frac{16.9151}{\Delta(s)} \cdot (s + 4.8012)(s + 4.7391)(s + 0.4426)(s + 0.2906) \cdot (s + 0.0769) \quad (34)$$

$$G_{1w}(s) = \frac{33.9492}{\Delta(s)} \cdot (s + 4.7125)(s + 4.4833)(s + 4.1978)(s + 0.4537) \cdot (s + 0.2511)(s + 0.0769) \quad (35)$$

$$G_{2w}(s) = \frac{-2.0609}{\Delta(s)} \cdot (s + 4.9144)(s + 4.4833)(s + 4.1978)(s + 0.4537) \cdot (s + 0.0803)(s - 245.3980) \quad (36)$$

$$G_{3w}(s) = \frac{-9.1034}{\Delta(s)} \cdot (s + 221.193)(s + 4.4833)(s + 4.1978)(s + 0.3341) \cdot (s + 0.0248) \quad (37)$$

$$G_{4w}(s) = \frac{-6.2342}{\Delta(s)} \cdot (s + 226.687)(s + 4.4833)(s + 4.1978) \cdot (s + 2.4009 + j \cdot 0.1376)(s + 2.4009 - j \cdot 0.1376) \cdot (s + 0.5219 + j \cdot 0.4202)(s + 0.5219 - j \cdot 0.4202) \cdot (s + 0.3235)(s + 0.04734) \quad (38)$$

where

$$\Delta(s) = (s + 226.6870)(s + 4.4833)(s + 4.1978)(s + 2.7323) \cdot (s + 1.8551)(s + 0.3285) \cdot (s + 6.9533 + j \cdot 0.2716)(s + 6.9533 - j \cdot 0.2716) \cdot (s + 0.0655 + j \cdot 0.0486)(s - 0.0655 + j \cdot 0.0486)$$

III.1 Design Objective:

The design task is to find a controller that keeps the four output signals, the controller variable and its rate within the following bounds for all times $t \in [0, \infty)$:

$$\beta_u = 37.01 \geq |u(t)| \quad (39)$$
$$\beta_{\dot{u}} = 0.75 \geq |\dot{u}(t)| \quad (40)$$
$$\beta_1 = 0.1 \geq |y_1(t)| \quad (41)$$
$$\beta_2 = 65.27 \geq |y_2(t)| \quad (42)$$
$$\beta_3 = 5.55 \geq |y_3(t)| \quad (43)$$
$$\beta_4 = 2.86 \geq |y_4(t)| \quad (44)$$

III.2 Design Execution:

Since bandwidth was not a concern in Parlos et al. [1988], y_2 is arbitrarily chosen for feedback. A family of closed loop circles (Table 1) as in section II can be determined. Its common intersection area displays the necessary location for any valid closed loop transfer function $L_c(s)$. The optimal value for α was

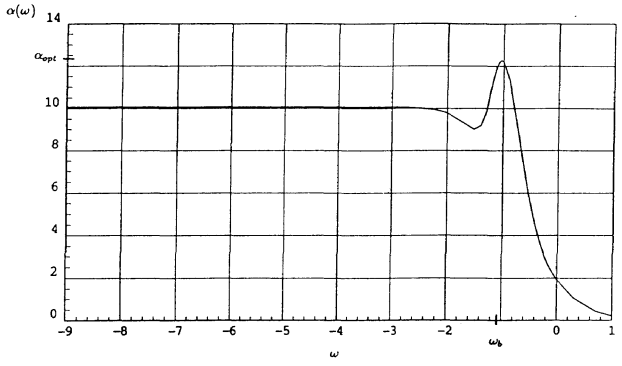

Fig. 8. Optimal Values for α over the frequency ω

found at the binding frequency $\omega_b = 0.092s^{-1}$ with $\alpha_{opt} = 12.27$ equivalent to a disturbance of 8.15%, where the area shrinks to a single point (Fig. 8). With $\alpha_{design} = \alpha_{opt}$ bounds on magnitude and phase for a valid closed loop transfer function, $L_c(s)$ are plotted over the entire frequency range (Fig. 9). Assume there is an $L_c(s)$ that meets both magnitude and phase bounds. If the transfer function corresponding to the saturating constraints (4 - 8) has an oscillatory step response without undershoot, a step is not the worst possible disturbance, but a square wave, as mentioned in sections I and II. Thus the theoretical maximum disturbance that can be rejected by this system is less than 8.15%. If the system has an undershoot however, the allowed disturbance might be even greater, since these systems

relax the frequency bound (section II.2) and the effects cancel each other out. In the best case ($\gamma = 4$) a step disturbance of height 32.6% can be rejected. But since this can occur only with an undershoot an appropriate square wave that violates the constraints can be found. Thus, 32.6% is a conservative upper bound for the maximal allowable size of the persistent disturbance. Only if the step response has neither undershoot nor overshoot is 8.15% the maximum disturbance that can be rejected satisfying all imposed time domain constraints.

A closed loop transfer function $L_c(s)$ that meets magnitude and phase bounds for 8.15% could not be determined easily. The best result found was for $\alpha_{design} = 6.87\%$ with

$$L_c'(s) = -3.33 \cdot \frac{s^2}{(s+0.063)^2 \cdot (s+10)^3 \cdot (s+100)^2} \qquad (45)$$

Using $L_o(s) = \frac{L_c(s)}{1-L_c(s)}$ and (6) the controller $G_c(s)$ can be computed:

$$\begin{aligned} G_c(s) = -0.000098 \cdot & \\ & \frac{(s+226.6900)(s+4.4833)(s+4.1978)(s+2.7323)}{(s+2.4614+j\cdot 0.1197)(s+2.4614-j\cdot 0.1197)} \cdot \\ & \frac{(s+0.6953+j\cdot 0.2716)(s+0.6953-j\cdot 0.2716)}{(s+0.4676+j\cdot 0.2985)(s+0.4676-j\cdot 0.2985)} \cdot \\ & \frac{(s+0.0656+j\cdot 0.0486)(s+0.0656-j\cdot 0.0486)}{(s+0.0472+j\cdot 0.0273)(s+0.0472-j\cdot 0.0273)} \cdot \\ & \frac{(s+1.8551)(s+0.3285)s^2}{(s+6.1285+j\cdot 6.1260)(s+6.1285-j\cdot 6.1260)} \cdot \\ & \frac{1}{(s+0.0769)(s+0.0074)(s+17.9280)} \cdot \\ & \frac{1}{(s+97.7790)(s+102.0700)} \end{aligned} \qquad (46)$$

$L_c'(s)$ saturates at $\omega = 0.01 s^{-1}$ the magnitude bound at the constraint for y_4 (Fig. 10). The time domain simulations (Figs. 11- 16) confirm that y_4 is saturated, too. Therefore the assumption $\gamma = 1$ for the transfer function $\frac{y_4(s)}{W(s)}$ is justified (section II.2). The signal is oscillatory however, and an appropriate

Operating Point	Disturbance	
	Theoretical Max. $(\frac{100}{\alpha_{opt}})$	Achieved Value
10%	3.73%	1.32%
20%	4.75%	2.27%
50%	6.68%	4.11%
70%	7.50%	4.94%
90%	8.15%	6.87%
100%	8.44%	6.89%
110%	8.68%	6.61%

Table 5: Allowable Disturbances at All Operating Points ($\gamma = 1$)

square wave can violate the time bound $|y_4(t)| \leq \beta_4$, for which the actual allowed disturbance is less than 6.87%.

Table 5 summarizes the results for all operating points. The column termed "Theoretical Max.$(\frac{100}{\alpha})$" shows the maximum

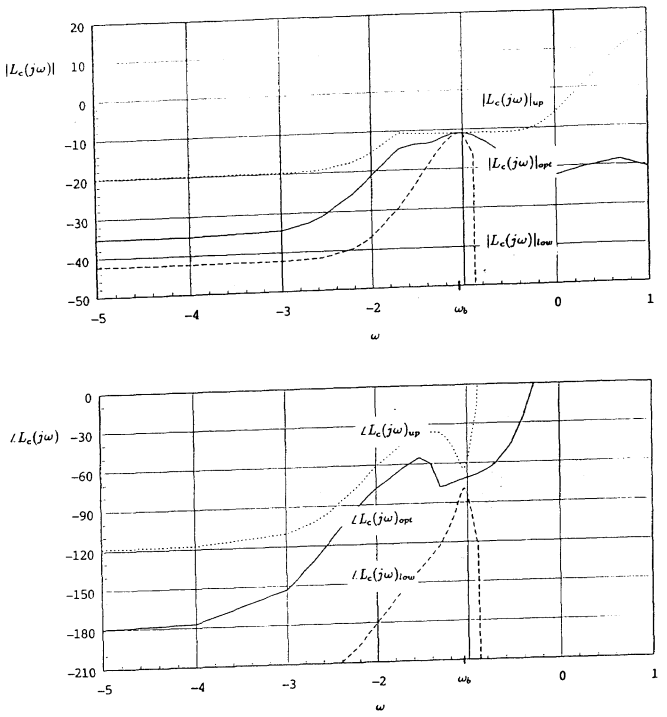

Fig. 9. Bounds on Magnitude and Phase for a Valid $L_c(s)$ for $\alpha_{design} = \alpha_{opt}$

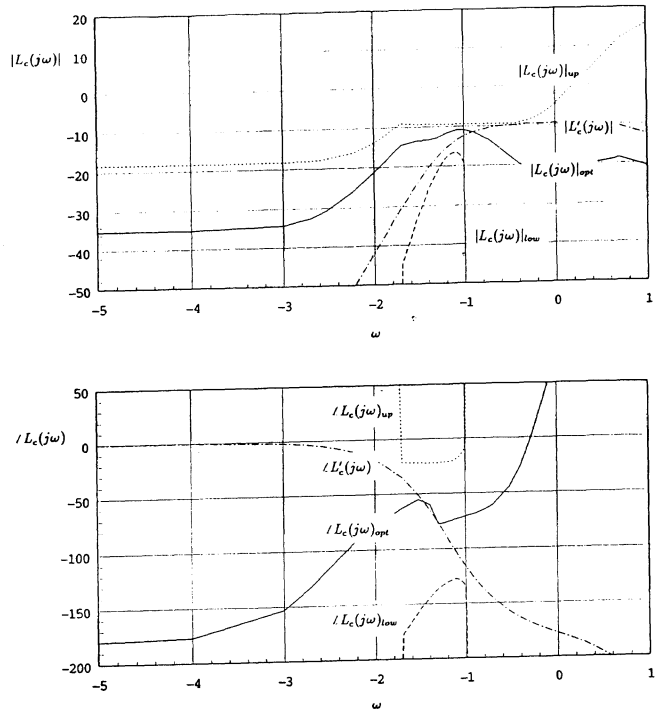

Fig. 10. Bounds on Magnitude and Phase for $L_c'(s)$ for 6.87% Tolerable Disturbance

disturbance at each operating point that yields the smallest possible common area of intersection over the entire frequency range. The column "Achieved Value" shows the required value for $\frac{100}{\alpha}$ so that the area of common intersection includes the specific closed loop transfer function $L_c'(s)$. Clearly, the val-

Operating Point	Maximum Disturbance
10%	2.19%
20%	3.10%
50%	4.29%
70%	5.29%
90%	6.87%
100%	6.29%
110%	7.17%

Table 6: Allowable Disturbances at All Operating Points ($\gamma \geq 1$)

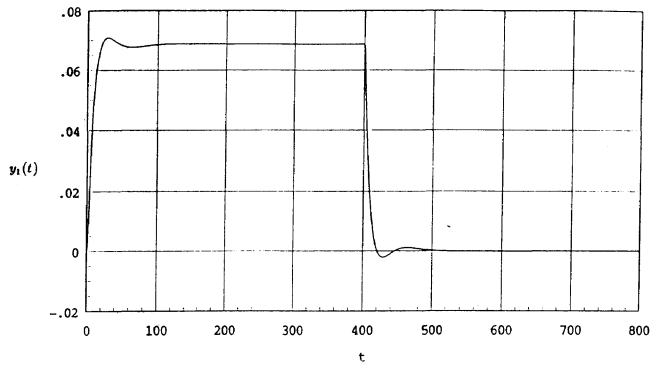

Fig. 11. Step Response of y_1 for 6.87% Tolerable Disturbance

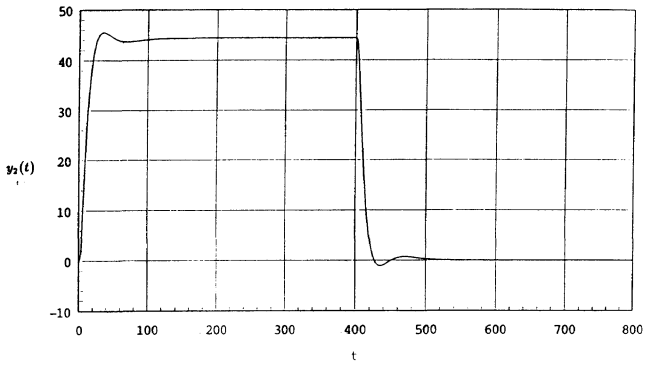

Fig. 12. Step Response of y_2 for 6.87% Tolerable Disturbance

ues of the second column are always smaller than to those of the first column. Remember that γ was assumed to be 1. But the time domain simulations at the operating points 10%, 20%, 50%, 70% and 110% display that the actual step height is even greater, since the time domain bounds are not saturated. This means, that in these cases γ is greater than 1, relaxing the frequency domain bound and enlarging the allowed region.

Table 6 shows the achieved values for the maximum step height at each operating point using the true value for γ that yields time domain bound saturation.

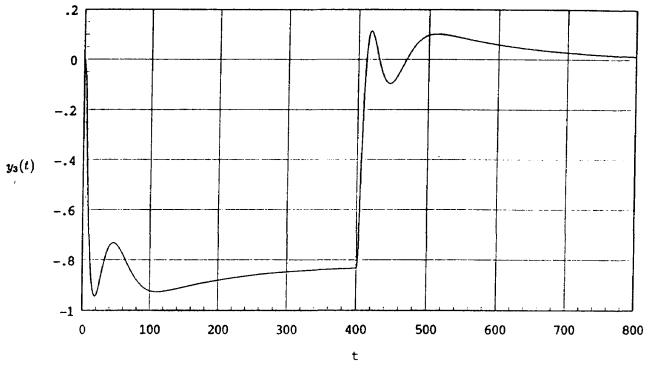

Fig. 13. Step Response of y_3 for 6.87% Tolerable Disturbance

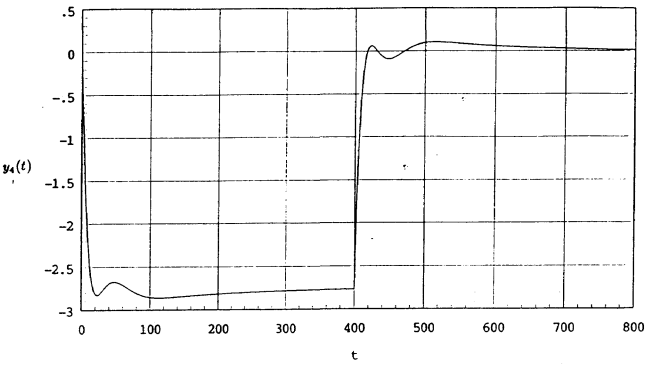

Fig. 14. Step Response of y_4 for 6.87% Tolerable Disturbance

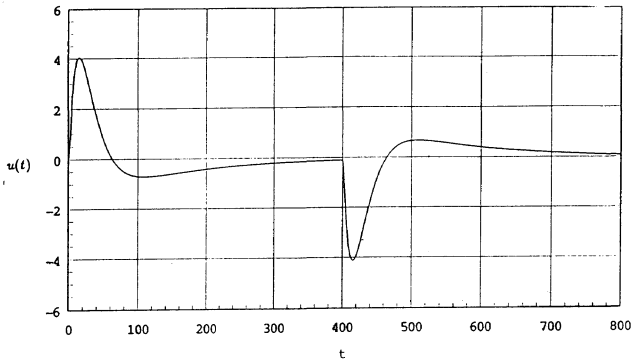

Fig. 15. Step Response of u for 6.87% Tolerable Disturbance

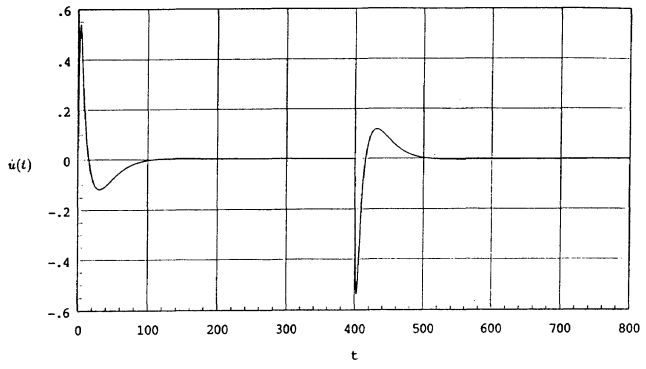

Fig. 16. Step Response of $\dot{u}$ for 6.87% Tolerable Disturbance

IV. CONCLUSIONS

A frequency domain design methodology was presented that directly imposes time domain constraints on output signals and the control variable under an unknown-but-bounded disturbance.

In the loop shaping procedure, bandwidth considerations can be incorporated simultaneously. The approach can easily be extended to plant uncertainty by formulating the frequency bounds just for the nominal plant. Since the allowed region in the closed loop plane is concave, only the edge points of the uncertainty region must be checked; if they are in the allowed region over the entire frequency range, the time domain constraints are also met for the uncertain plant.

The efficency of the method can be improved with an algorithm that optimizes the allowed disturbance while guaranteeing that the output and the controller transfer functions have a nonoscillatory step response. Therefore criteria must be developed to specify the largest class of transfer functions with this particular behavior. Transfer functions with oscillatory step responses can also be included in the methodology by introducing a factor δ that relates the highest possible output signal obtained by an appropriate square wave to a step response.

REFERENCES

1. Franchek, M.A.,"Synthesis of Controllers for Prespecified Performance in Linear Uncertain Systems,"*MS Thesis*, Department of Mechanical Engineering, Texas A&M University, College Station, Texas, December 1988.

2. Jayasuriya, S., and Franchek, M.A., "Loop Shaping for Robust Performance in Systems with Structured Perturbations," *ASME Paper Number 88-WA/DSC-11, presented at the ASME Winter Annual Meeting*, Chicago, Illinois, December 1988.

3. Jayasuriya, S., and Franchek, M.A., "Frequency Domain Design for Prespecified State and Control Constraints under Persistent Bounded Disturbances," *Proceedings of the IEEE Conference in Decision and Control*, Austin, Texas, December 1988.

4. Jayasuriya, S., Zentgraf, P., and Rabins, M.,"On Maximizing the Size of a Persistent Bounded Disturbance," *submitted for presentation at the IFAC World Congress*, Tallin, USSR, July 1990.

5. Normiatsu, T., and Ito, M., "On the Zero Non-Regular Control System,"*J. Institute Electrical Engineering Japan*, Vol. 81, pp. 556-575, 1961.

6. Parlos, A. G., et al., "Non-Linear Multivariable Control of Power Plants Based on the Unknown-But-Bounded Disturbance Model,"*IEEE Trans. Automatic Control*, Vol. AC-31, pp. 527-534, June 1986.

7. Zentgraf, P.,"An Automation of a Frequency Domain Controller Design Methodology," *Project Report*, Department of Mechanical Engineering, Texas A&M University, College Station, Texas, April 1989a.

8. Zentgraf, P.,"Controllers for Maximizing Allowable Disturbances subject to System Constraints," *Diploma Thesis*, Department of Mechanical Engineering, Texas A&M University, College Station, Texas, August 1989b.